Modified Regional Self-Interaction Correction Method Based on the Pseudospectral Method

ARTICLE *in* THE JOURNAL OF PHYSICAL CHEMISTRY A · AUGUST 2010

Impact Factor: 2.69 · DOI: 10.1021/jp909915d · Source: PubMed

3 AUTHORS, INCLUDING:

Ayako Nakata
National Institute for Materials Science
17 PUBLICATIONS **246** CITATIONS
SEE PROFILE

Takao Tsuneda
University of Yamanashi
68 PUBLICATIONS **3,924** CITATIONS
SEE PROFILE

Modified Regional Self-Interaction Correction Method Based on the Pseudospectral Method†

Ayako Nakata, Takao Tsuneda,* and Kimihiko Hirao

Next-generation Molecular Theory Unit, Advanced Science Institute, RIKEN, Saitama 351-0198, Japan, and CREST, Japan Science and Technology Agency, Saitama 332-0012, Japan

Received: October 16, 2009; Revised Manuscript Received: December 11, 2009

A modification of the regional self-interaction correction (RSIC) scheme (Tsuneda et al., *J. Comput. Chem.* **2003**, *24*, 1592), pseudospectral RSIC (PSRSIC), is proposed to eliminate the self-interaction errors (SIEs) especially in core regions. PSRSIC reduces the SIEs by substituting the HF exchange energy density calculated with the use of the pseudospectral technique for the exchange energy in the SI-domain region. PSRSIC is combined with the long-range correction (LC) scheme. TDDFT calculations with LC-PSRSIC yield all of the core-, valence-, Rydberg-, and charge-transfer-excitation energies with reasonable accuracy. Core-ionization energies are also well-reproduced by LC-PSRSIC.

Introduction

Core excitations of molecules are of experimental and theoretical interest because these excitations provide important information about molecular structures and dynamics. Extended X-ray absorption fine structure (EXAFS) measurement of absorption spectra of core excitations to the continuum state is a standard procedure for obtaining information on bond lengths, etc. On the other hand, most of the core-excitation-energy calculations have been carried out by using high-level wave function-based correlation methods, e.g., multiconfigurational quasidegenerate perturbation theory (MCQDPT)[1] and symmetry adapted cluster configuration interaction (SAC-CI),[2−4] although they require large computational time. This is because high-accuracy methods are needed for describing high excitation levels. Time-dependent density functional theory (TDDFT)[5−12] gives accurate excitation energies in much less computational time than high-level wave function calculations take. However, TDDFT calculations with conventional functionals significantly underestimate core-excitation energies.[13−15]

The underestimation of the core-excitation energies is suggested to be due to the self-interaction error (SIE)[15] that originates from the error in the self-exchange energy of the exchange functional. Several techniques including a self-interaction correction (SIC) have been proposed to improve on the core-excitation energies of TDDFT. As far as we know, most of the related techniques have concentrated on increasing the portion of the Hartree−Fock (HF) exchange integral for the core regions in comparison with that for valence regions to decrease SIE while maintaining accuracy for valence excitations. For example, core−valence B3LYP (CV−B3LYP)[16−18] and core−valence−Rydberg B3LYP (CVR−B3LYP)[19,20] use 50% of the HF exchange for core orbitals and 20% of the HF exchange for valence orbitals and get core-excitation energies within about 1 eV of the actual values. The long-range correction (LC) approach[21,22] including a short-range Gaussian attenuation (LCgau)[23] is based on this strategy.

Tsuneda and co-workers proposed another SIC approach, i.e., regional SIC (RSIC).[24] In RSIC, the exact exchange self-interaction (SI) energy of a 1s hydrogen-like atomic orbital is substituted for the exchange functional in the regions where the SI is dominant. For several reactions, RSIC gave more accurate energies for reaction barriers that had been underestimated in DFT calculations due to SIE. However, it hardly affects the core-excitation energies of the TDDFT calculations.[25] To overcome this problem, we recently proposed a modified RSIC (mRSIC) technique,[25] which takes into account the neglected energy contributions from 2s and higher atomic orbitals and reduces the sensitivity to the poor cusp behavior of the Gaussian basis functions. mRSIC reproduced core-excitation energies with reasonable accuracy, but it gave poor core-ionization energies and often caused the self-consistent field process not to converge.[25]

In this study, we developed a new RSIC method based on the pseudospectral technique to obtain accurate results for both core-excitation and core-ionization energies. In the new method, the exchange energies in the SI regions are calculated using the HF exchange energies instead of the exact exchange energies of hydrogen-like atomic orbitals. We presume that the poor core-ionization energies and unstable SCF convergence of mRSIC are due to the lack of interactions between the core and other orbitals. In the next section, we briefly review RSIC and mRSIC and describe the new method, pseudospectral RSIC (PSRSIC). In the third section, the accuracies of the new method are assessed by calculating the core-excitation and core-ionization energies. The final section concludes with a discussion of the advantages and disadvantages of this new method.

Theoretical Aspects

Regional Self-Interaction Correction (RSIC) and Modified RSIC (mRSIC) Methods. As mentioned in the previous studies,[26,27] the kinetic energy density τ of electrons in the SI regions, where electrons interact only with themselves, should be identical to the Weizsäcker kinetic energy density τ^W

† Part of the "Klaus Ruedenberg Festschrift".

* Corresponding author. Tel.: +81-48-462-1694. Fax: +81-48-462-1552. E-mail address: tsuneda@riken.jp.

10.1021/jp909915d
Published on Web 01/25/2010

$$\tau_\sigma \rightarrow \tau_\sigma^{\mathrm{W}} = \frac{|\nabla\rho_\sigma|^2}{4\rho_\sigma} \tag{1}$$

where ρ_σ is the σ-spin electron density. Making use of eq 1, we can identify the SI regions by calculating the ratio of τ_σ to τ_σ^{W}

$$t_\sigma = \frac{\tau_\sigma^{\mathrm{W}}}{\tau_\sigma} \quad (0 < t_\sigma \leq 1) \tag{2}$$

The RSIC method employs a partition function to cut out the SI regions

$$f_\sigma = \frac{1}{2}\left(1 + \mathrm{erf}\left[\frac{5(t_\sigma - a)}{1 - a}\right]\right) \quad (0 < a < 1) \tag{3}$$

where a is a parameter to control the size of the SI regions. Using this partition function, the SIC exchange energy density $\varepsilon_x^{\mathrm{SIC}}$ can be written as

$$\varepsilon_{x\sigma}^{\mathrm{SIC}}(\mathbf{r}) = f_\sigma\varepsilon_{x\sigma}^{\mathrm{SI}}(\mathbf{r}) + (1 - f_\sigma)\varepsilon_{x\sigma}^{\mathrm{DFT}}(\mathbf{r}) \tag{4}$$

where $\mathbf{r}$ is the radius vector from a nucleus to the center of paired-electron positions. In eq 4, $\varepsilon_x^{\mathrm{DFT}}$ is the exchange energy density of an exchange functional, and $\varepsilon_x^{\mathrm{SI}}$ is the self-exchange energy density, which is the exchange energy density of SI electrons.

For the self-exchange energy density, RSIC uses the exact SI energy density of the 1s orbital of a hydrogen-like atom

$$\varepsilon_{x\sigma}^{\mathrm{SI}}(\mathbf{r}) = -\frac{1}{2r}[1 - (1 + \alpha r)e^{-2\alpha r}] \tag{5}$$

where α is

$$\alpha = \frac{|\nabla\rho_\sigma|}{2\rho_\sigma} \tag{6}$$

The mRSIC method also takes into account the self-exchange energy densities of 2s and higher atomic orbitals. Furthermore, instead of using α in eq 6, the exchange energy for each orbital is calculated by using the nuclear charge of the central atom Z. For example, the exchange energy densities of 1s − 2p orbitals are given as follows

$$\begin{aligned}
\varepsilon_x^{1\mathrm{s}}(\mathbf{r}) &= -\frac{1}{2r}[1 - (1 + Zr)\mathrm{e}^{-2Zr}] \\
\varepsilon_x^{2\mathrm{s}}(\mathbf{r}) &= -\frac{1}{2r}\left[1 - \left(1 + \frac{3}{4}Zr + \frac{1}{4}Z^2r^2 + \frac{1}{8}Z^3r^3\right)e^{-Zr}\right] \\
\varepsilon_x^{2\mathrm{p}}(\mathbf{r}) &= -\frac{1}{2r}\left[1 - \left(1 + \frac{3}{4}Zr + \frac{1}{4}Z^2r^2 + \frac{1}{24}Z^3r^3\right)e^{-Zr}\right]
\end{aligned} \tag{7}$$

The total $\varepsilon_x^{\mathrm{SI}}$ is calculated as a linear combination of the atomic exchange energy densities ε_x^i in eq 7 with the electron densities of hydrogen-like atomic orbitals ρ_{H}^i,

$$\varepsilon_{x\sigma}^{\mathrm{SI}}(\mathbf{r}) = \sum_i^{n_\sigma} \rho_{\mathrm{H}}^i(\mathbf{r})\varepsilon_x^i(\mathbf{r}) \tag{8}$$

where n_σ corresponds to the occupied σ-spin atomic orbitals. The electron densities for $i = 1\mathrm{s} - 2\mathrm{p}$ are

$$\begin{aligned}
\rho_{\mathrm{H}}^{1\mathrm{s}}(\mathbf{r}) &= \frac{Z^3}{\pi}\mathrm{e}^{-2Zr} \\
\rho_{\mathrm{H}}^{2\mathrm{s}}(\mathbf{r}) &= \frac{Z^3}{32\pi}(2 - Zr)^2e^{-Zr} \\
\rho_{\mathrm{H}}^{2\mathrm{p}}(\mathbf{r}) &= \frac{Z^5}{96\pi}r^2e^{-Zr}
\end{aligned} \tag{9}$$

The derivations of ε_x^i and ρ_{H}^i are described in the previous paper.[25] It should be noted that $\varepsilon_x^{\mathrm{SI}}$ in eq 8 does not depend on the electron density ρ_σ, which is obtained from the molecular orbitals (MOs) composed of Gaussian basis functions. Therefore, we take the partial derivatives of $\varepsilon_x^{\mathrm{SI}}$ with respect to ρ_σ and its gradient $\nabla\rho_\sigma$. These partial derivatives seem to make it difficult for the SCF calculations to converge.

Pseudospectral RSIC Method. To overcome the problems of the mRSIC method, we shall use the HF exchange energy as the self-exchange energy density. The HF exchange energy is usually calculated by analytical integration with respect to $\mathbf{r}_1$ and $\mathbf{r}_2$ as

$$E_{\mathrm{HF}x} = -\frac{1}{4}\sum_{\mu\nu\lambda\kappa}\mathbf{P}_{\mu\nu}\mathbf{P}_{\lambda\kappa}\int\int\frac{\chi_\nu^*(\mathbf{r}_1)\chi_\lambda(\mathbf{r}_1)\chi_\kappa^*(\mathbf{r}_2)\chi_\mu(\mathbf{r}_2)}{|\mathbf{r}_1 - \mathbf{r}_2|}d\mathbf{r}_1d\mathbf{r}_2 \tag{10}$$

where $\mathbf{P}$ is a density matrix, and χ's are atomic orbitals with indices μ, ν, λ, and κ. Therefore, we have to determine the HF-exchange energy density in each region, and the pseudospectral (PS) technique[28,29] is available for this purpose. In the PS technique, the analytical integration is performed only for $\mathbf{r}_2$, and numerical quadrature is done for $\mathbf{r}_1$

$$E_{\mathrm{HF}x} = -\frac{1}{4}\sum_g^{N_{\mathrm{grid}}}\sum_{\mu\nu\lambda\kappa}\mathbf{P}_{\mu\nu}\mathbf{P}_{\lambda\kappa}\chi_\nu^*(\mathbf{r}_g) \times \chi_\lambda(\mathbf{r}_g)\int\frac{\chi_\kappa^*(\mathbf{r}_2)\chi_\mu(\mathbf{r}_2)}{|\mathbf{r}_2 - \mathbf{r}_g|}d\mathbf{r}_2 \tag{11}$$

For this energy, the self-exchange energy density becomes

$$\varepsilon_x^{\mathrm{SI}}(\mathbf{r}) = -\frac{1}{4}\sum_{\mu\nu\lambda\kappa}\mathbf{P}_{\mu\nu}\mathbf{P}_{\lambda\kappa}\chi_\nu^*(\mathbf{r}) \times \chi_\lambda(\mathbf{r})\int\frac{\chi_\kappa^*(\mathbf{r}_2)\chi_\mu(\mathbf{r}_2)}{|\mathbf{r}_2 - \mathbf{r}|}d\mathbf{r}_2 \tag{12}$$

The SIC exchange energy density is obtained by substituting this energy density for $\varepsilon_x^{\mathrm{SI}}$ into eq 4. We would like to emphasize that PSRSIC calculations require no orbital localization procedure for the unitary invariance of the orbital-dependent HF exchange integral because the generalized Kohn−Sham self-consistent field calculations[30,31] are carried out using the functional derivative of PSRSIC.

The PSRSIC method is similar to the local hybrid (LH) method of Jaramillo et al.,[32,33] despite that these methods came from different ideas. Their LH method also uses the ratio t in eq 2 as an indicator of one-electron regions. The exchange

energy density is calculated using the localized HF implementation of Della Sala and Görling[34] in the LH method. Several partition functions using t have been reported for the LH method: e.g., $f = t$,[32] $0.48t$,[35] and $(1 - \Pi)^{\xi}t^{\gamma}$,[36] where Π is the "density matrix similarity metric"[37] and ξ and γ are parameters.[36] However, as described later, the LH method unfortunately gives poor core-excitation energies. This is in contrast to the PSRSIC method, which gives accurate core-excitation energies by using TDDFT calculations and yet maintains the accuracy of the core-ionization-energy calculations.

Combination of PSRSIC Method with LC Scheme. Besides underestimating the core-excitation energies, the usual TDDFT calculations also underestimate charge-transfer- and Rydberg-excitation energies and the oscillator strengths. It has been reported that TDDFT calculations using the LC scheme do not show such underestimations and further provide accurate valence-excitation energies.[21,22] Therefore, to provide a whole range of excitation spectra, one of the best strategies is to optimize the PSRSIC method for its combination with this LC-TDDFT.

In the LC scheme, the two-electron operator is divided into short- and long-range parts

$$\frac{1}{r_{12}} = \frac{1 - \mathrm{erf}(\mu r_{12})}{r_{12}} + \frac{\mathrm{erf}(\mu r_{12})}{r_{12}} \tag{13}$$

where r_{12} is an electron−electron distance and μ is the only parameter (for BOP functional mentioned later, μ is optimized as 0.33 for ground-state calculations[22] and 0.47 for excited-state calculations[23]). In the LC-PSRSIC method, the HF exchange integral is adapted to the long-range part of the exchange functional as usual, and PSRSIC is performed only for the short-range part. The short-range part of the exchange energy is given by

$$\varepsilon_{x\sigma}^{\text{SR-SIC}}(\mathbf{r}) = f_\sigma \varepsilon_{x\sigma}^{\text{SR-SI}}(\mathbf{r}) + (1 - f_\sigma)\varepsilon_{x\sigma}^{\text{SR-DFT}}(\mathbf{r}) \tag{14}$$

The short-range DFT exchange energy $\varepsilon_x^{\text{SR-DFT}}$ in eq 14 is described as

$$\varepsilon_x^{\text{SR-DFT}} = -\frac{1}{2}\sum_\sigma \rho_\sigma^{4/3} K_\sigma \left\{1 - \frac{8}{3}a_\sigma\left[\sqrt{\pi}\,\mathrm{erf}\left(\frac{1}{2a_\sigma}\right) + (2a_\sigma - 4a_\sigma^3)\exp\left(-\frac{1}{4a_\sigma^2}\right) - 3a_\sigma + 4a_\sigma^3\right]\right\} \tag{15}$$

where

$$a_\sigma = \frac{\mu K_\sigma^{1/2}}{6\sqrt{\pi}\rho_\sigma^{4/3}} \tag{16}$$

In eqs 15 and 16, K_σ is the GGA part of the exchange functional, and for PSRSIC, it is expressed as

$$K_\sigma(\mathbf{r}) = -2\rho_\sigma^{-4/3}(1 - f_\sigma)\varepsilon_{x\sigma}^{\text{DFT}}(\mathbf{r}) \tag{17}$$

The short-range self-exchange energy density $\varepsilon_x^{\text{SR-SI}}$ requires the short-range HF exchange integral to be calculated at each position. The conventional $(ss|ss)$-type integral is given by

$$(ss|ss) = D_{\text{IJ}}D_{\text{KL}}\frac{2\pi^{5/2}}{(pq)^{3/2}\alpha^{-1/2}}F_0(\alpha r_{\text{PQ}}^2) \tag{18}$$

where F_0 is the Boys function, α is defined as

$$\alpha = \left(\frac{1}{p} + \frac{1}{q}\right)^{-1} \tag{19}$$

and D_{IJ} is a constant factor given by

$$D_{\text{IJ}} = \exp\left(-\frac{ij}{i+j}r_{\text{IJ}}^2\right) \tag{20}$$

The production of two s-type Gaussian functions centered at I and J with exponents i and j (K and L with k and l) is contracted to a single Gaussian function centered at P(Q) with the exponent $p(q)$. The short-range $(ss|ss)$-type integral $(ss|ss)_\mu$, in which $1/r_{12}$ is replaced by the error function $\mathrm{erf}(\mu r_{12})/r_{12}$, is the same as that of the $(ss|ss)$ integral except for α[38]

$$(ss|ss)_\mu = D_{\text{IJ}}D_{\text{KL}}\frac{2\pi^{5/2}}{(pq)^{3/2}\alpha_\mu^{-1/2}}F_0(\alpha_\mu r_{\text{PQ}}^2) \tag{21}$$

$$\alpha_\mu = \left(\frac{1}{p} + \frac{1}{q} + \frac{1}{\mu^2}\right)^{-1} \tag{22}$$

Analytical integrations are performed with respect to both $\mathbf{r}_1$ and $\mathbf{r}_2$ in eqs 18 and 21. In the PSRSIC method, the analytical integration is performed only for $\mathbf{r}_1$, and the $(ss|ss)$- and $(ss|ss)_\mu$-type integrals are written as

$$(ss|ss) = D_{\text{IJ}}D_{\text{KL}}\frac{2\pi}{p}\int \exp(-qr_{2\text{Q}}^2)F_0(pr_{2\text{P}}^2)d\mathbf{r}_2 \tag{23}$$

$$(ss|ss)_\mu = D_{\text{IJ}}D_{\text{KL}}\frac{2\pi\mu}{p\sqrt{p+\mu^2}} \times \int \exp(-qr_{2\text{Q}}^2)F_0\left(\left(\frac{1}{p} + \frac{1}{\mu^2}\right)^{-1}r_{2\text{P}}^2\right)d\mathbf{r}_2 \tag{24}$$

Consequently, the short-range self-exchange energy density at each position is calculated by the numerical integration of eq 24 over $\mathbf{r}_2$ in the PSRSIC method.

Computational Details

The excitation-energy calculations of typical molecules were performed by using the time-dependent Kohn−Sham method with cc-pVTZ[39] and Dunning−Hay single (s, p) Rydberg (cc-pVTZr) basis functions.[40] For core-ionization-energy calculations, we used the Δ-KS technique[41,42] with the cc-pVTZr basis functions. In the present calculations, we used no splitting core basis functions such as cc-pCVTZ because it has been reported that the effect of core splitting is only about 0.1 eV for second-row atoms.[16] In the numerical integrations of (short-range) exchange-correlation functionals, 96 radial points in the Euler−Maclaurin quadrature[43] and 12 × 24 angular points in the Gauss−Legendre quadrature[44] were adopted.

The Becke 1988 exchange functional[45] was employed as $\varepsilon_x^{\text{DFT}}$ in eq 4 with the one-parameter progressive correlation func-

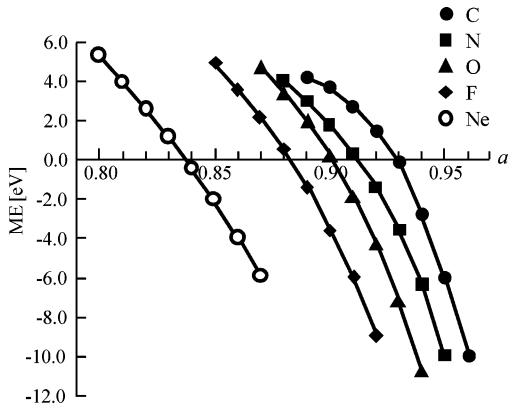

Figure 1. Mean errors (MEs) of the 1s core-excitation energies calculated by LC-PSRSIC plotted in terms of parameter *a* for various atoms.

tional[46] (BOP) in the LC calculations (LC-PSRSIC, LC-mRSIC, and LC-BOP). For comparison, we used the hybrid B3LYP[47,48] functional. We also examined the LH method with $t = 1$ (LH(1))[32] and $t = 0.48$ (LH(0.48))[35] with the use of the LC scheme. The BOP functional was used in the LH calculations, whereas the LDA functional was used in the original study.[32,35] Note that LC-PSRSIC calculations using the BLYP functional gave very close results to BOP ones within the difference of 0.1 eV.

For simplicity, we employed an approximate TDDFT formalism for LC-PSRSIC and LC-mRSIC (see Appendix). In this approximation, the LC-TDBOP equation with the orbital energies and coefficients of LC-PSRSIC and LC-mRSIC is used in the TDDFT calculations.[25] This approximation assumes that the contributions from PSRSIC and mRSIC to the off-diagonal elements are negligible compared to the contributions to the diagonal elements in the TDDFT matrix.[8,16−20] The same approximation was applied to the LH(1) and LH(0.48) methods. We also neglected relativistic effects because we calculated only light molecules in the present calculations. All calculations were performed with a development version of GAMESS ver. 2008.[49,50]

Results and Discussion

Determination of Parameter *a*. Before the test calculations, we have to determine the parameter *a* of LC-PSRSIC in eq 3, which controls the range of SI regions. Figure 1 plots the mean errors (MEs) in calculated core-excitation energies from X-1s orbitals (X = C of $\mathbf{C}_2H_4$ and $\mathbf{C}O_2$, N of $\mathbf{N}_2$ and $\mathbf{N}H_3$, O of $C\mathbf{O}_2$ and $H_2\mathbf{O}$, F of H**F** and $\mathbf{F}_2$, and Ne) in terms of parameter *a* for each atom (see Supporting Information for the values of the excitation energies and MEs). As the figure shows, the TDDFT core-excitation energies calculated with LC-PSRSIC depend on *a*: the MEs vary more than 10 eV for every atom. Figure 1 also indicates that the optimized value of *a* corresponding to the intersection of the *x*-axis and the interpolation varies for each atom. This may be due to that the range of SI regions significantly depends on the atomic species. Therefore, we

TABLE 1: 1s Core-Excitation Energies (in eV) of C_2H_2, C_2H_4, N_2, NH_3, CH_2O, H_2O, and HF Molecules and Ne Atom Calculated by TDDFT with BOP, LC-BOP, LC-mRSIC, LC-PSRSIC, B3LYP, and LH Functionals with cc-pVTZ Plus Rydberg Basis Functions[a]

molecule	assignment	BOP	LC-BOP	LC-mRSIC	LC-PSRSIC	B3LYP	LC-LH(1)	LC-LH(0.48)	exptl
C_2H_2	C1s → π^*	269.7 (−16.1)	269.7 (−16.1)	282.9 (−2.9)	284.9 (−0.9)	275.3 (−10.5)	297.1 (+11.3)	282.9 (−2.9)	285.8[b]
C_2H_4	C1s → 3sσ	269.4 (−17.7)	270.6 (−16.5)	284.5 (−2.6)	285.8 (−1.3)	275.9 (−11.2)	298.6 (+11.5)	284.6 (−2.5)	287.1[c]
N_2	N1s → π^*	382.4 (−18.6)	382.2 (−18.8)	402.8 (+1.8)	402.4 (+1.4)	388.6 (−12.4)	415.3 (+14.3)	398.1 (−2.9)	401.0[d]
NH_3	N1s → $3p_e$	381.2 (−21.1)	382.2 (−20.1)	400.7 (−1.6)	401.6 (−0.7)	388.8 (−13.5)	415.5 (+13.2)	398.8 (−3.5)	402.3[e]
CH_2O	O1s → π^*	509.4 (−21.4)	509.3 (−21.5)	534.5 (+3.7)	533.5 (+2.7)	516.8 (−14.0)	546.6 (+15.8)	527.3 (−3.5)	530.8[b]
H_2O	O1s → $3p_{b2}$	511.9 (−24.0)	512.4 (−23.5)	536.8 (+0.9)	536.7 (+0.8)	520.7 (−15.2)	551.0 (+15.1)	531.7 (−4.2)	535.9[e]
HF	F1s → σ^*	660.1 (−27.3)	660.3 (−27.1)	689.2 (+1.8)	688.6 (+1.2)	669.4 (−18.0)	702.4 (+15.0)	681.0 (−6.4)	687.4[f]
HF	F1s → 3p	661.6 (−29.2)	662.5 (−28.3)	691.5 (+0.7)	690.9 (+0.1)	671.6 (−19.2)	704.9 (+14.1)	683.4 (−7.4)	690.8[f]
Ne	Ne1s → $3p_{tu}$	831.5 (−35.6)	831.0 (−36.1)	865.7 (−1.4)	865.6 (−1.5)	842.9 (−24.2)	878.9 (+11.8)	855.2 (−11.9)	867.1[g]
MAE (total)[h]		23.4	23.1	1.9	1.2	15.4	13.6	5.0	

[a] Errors with respect to the experimental data are shown in parentheses. [b] Ref 51. [c] Ref 52. [d] Ref 53. [e] Ref 54. [f] Ref 55. [g] Ref 56. [h] Mean absolute errors from the experimental data.

TABLE 2: Valence- and Rydberg-Excitation Energies (in eV) of C_2H_2, C_2H_4, C_4H_6, CH_2O, and H_2O Molecules Calculated by TDDFT with BOP, LC-BOP, LC-mRSIC, LC-PSRSIC, B3LYP, and LH Functionals with cc-pVTZ Plus Rydberg Basis Functions[a]

molecule	state	BOP	LC-BOP	LC-mRSIC	LC-PSRSIC	B3LYP	LC-LH(1)	LC-LH(0.48)	exptl
					Valence → Valence excitations				
C_2H_2	$^1\Sigma_u^+$	6.86 (−0.24)	6.71 (−0.39)	6.60 (−0.50)	6.66 (−0.44)	6.75 (−0.35)	7.35 (+0.25)	6.96 (−0.14)	7.10[b]
C_2H_4	$^1B_{1u}$	7.23 (−0.77)	7.68 (−0.32)	7.58 (−0.42)	7.66 (−0.34)	7.44 (−0.56)	8.32 (+0.32)	8.03 (+0.03)	8.00[c]
C_4H_6	^1B_u	5.42 (−0.50)	5.93 (+0.01)	5.86 (−0.06)	5.92 (−0.00)	5.62 (−0.30)	6.42 (+0.50)	6.17 (+0.25)	5.92[d]
CH_2O	$^1A_2$	3.95 (+0.01)	3.90 (−0.04)	3.85 (−0.09)	3.83 (−0.11)	4.01 (+0.07)	5.22 (+1.28)	4.38 (+0.44)	3.94[c]
MAE[f]		0.38	0.19	0.27	0.22	0.32	0.59	0.21	
					Valence → Rydberg excitations				
C_2H_2	$^1\Sigma_g^+$	7.61 (−1.60)	8.63 (−0.58)	8.55 (−0.66)	8.67 (−0.54)	8.05 (−1.16)	10.33 (+1.12)	9.87 (+0.66)	9.21[b]
C_2H_4	$^1B_{3u}$	6.46 (−0.65)	7.25 (+0.14)	7.10 (−0.01)	7.29 (+0.18)	6.71 (−0.40)	8.49 (+1.38)	8.29 (+1.18)	7.11[c]
CH_2O	$^1B_2$	5.75 (−1.34)	6.75 (−0.34)	6.56 (−0.53)	6.75 (−0.34)	6.42 (−0.67)	8.60 (+1.51)	8.03 (+0.94)	7.09[c]
H_2O	$^1A_2$	7.66 (−1.44)	8.55 (−0.55)	8.46 (−0.64)	8.60 (−0.50)	7.57 (−1.53)	11.14 (+2.04)	10.16 (+1.06)	9.10[f]
MAE[f]		1.26	0.40	0.46	0.39	0.94	1.51	0.96	
MAE (total)[f]		0.82	0.30	0.36	0.31	0.63	1.05	0.59	

[a] Errors with respect to the experimental data are shown in parentheses. [b] Ref 57. [c] Ref 22. [d] Ref 58. [e] Ref 8. [f] Mean absolute errors from the experimental data.

TABLE 3: Charge-Transfer-Excitation Energies (in eV) of the C_2H_4—C_2F_4 Dimer for a Long Intermolecular Distance *R* (in Å) calculated by TDDFT with BOP, LC-BOP, LC-mRSIC, LC-PSRSIC, B3LYP, and LH Functionals with 6-31G* Basis Functions

R	BOP	LC-BOP	LC-mRSIC	LC-PSRSIC	B3LYP	LC-LH(1)	LC-LH(0.48)	exptl[a]
5.00	5.62	9.91	9.64	10.04	7.25	11.11	10.39	
6.00	5.67	10.43	10.16	10.56	7.40	11.65	10.92	
7.00	5.70	10.79	10.52	10.92	7.50	12.02	11.29	
8.00	5.71	11.06	10.79	11.19	7.57	12.30	11.56	
9.00	5.72	11.27	10.99	11.40	7.62	12.51	11.77	
10.00	5.73	11.44	11.16	11.56	7.66	12.68	11.93	
∞ (= c_0)	5.85	12.97	12.68	13.09	8.07	14.25	13.49	12.5
c_1 (au)	0.08	1.06	1.05	1.06	0.28	1.09	1.07	$\geq$1

[a] Ref 22.

TABLE 4: Oscillator Strengths ($\times 10^{-2}$) of Core, Valence, And Rydberg Excitations of a C_2H_4 Molecule by TDDFT with BOP, LC-BOP, LC-PSRSIC, and B3LYP Functionals with cc-pVTZ Plus Rydberg Basis Functions

transition	BOP	LC-BOP	LC-PSRSIC	B3LYP
C1s $\rightarrow \pi^*$	5.64	6.64	6.98	8.19
C1s $\rightarrow$ 3sσ	0.00	0.53	0.53	0.60
$\pi \rightarrow \pi^*$	20.87	34.47	35.02	27.82
$\pi \rightarrow$ 3sσ	7.10	9.29	9.07	8.00

determined *a* from a second-order least-mean-square (LMS) fit to the nuclear charge *Z*

$$a = b_1 Z^2 + b_2 Z + b_3 \tag{25}$$

where $b_1 = -0.00100$, $b_2 = -0.00648$, and $b_3 = 1.01083$. This is similar to what is done in mRSIC.[25] In the present study, *Z* was determined as the nuclear charge of the atom, to which each grid point belongs.

Core-Excitation-Energy Calculations. Using the optimized parameter *a* in eq 25, we assessed LC-PSRSIC in TDDFT core-excitation-energy calculations on several typical molecules. Tables 1 and 2 list the calculated excitation energies. These tables also display the results of BOP, LC-BOP, LC-mRSIC, B3LYP, LC-LH(1), and LC-LH(0.48) for comparison. The deviations from the experimental values are shown in parentheses.

Core-excitation energies were calculated for C_2H_2, C_2H_4, N_2, NH_3, CH_2O, H_2O, and HF molecules and the Ne atom (Table 1). As shown in the table, LC-PSRSIC gave very accurate core-excitation energies with a mean absolute error (MAE) of 1.2 eV. This MAE is smaller than that of LC-mRSIC, 1.9 eV. As shown in the previous study, SI-uncorrected BOP and LC-BOP significantly underestimated the core-excitation energies by more than 20 eV. The close MAEs, 23.4 eV for BOP and 23.1 eV for LC-BOP, indicate that long-range exchange interactions hardly affect core excitations in TDDFT calculations. In contrast, the hybrid B3LYP functional affected core-excitation energies and reduced MAE to 15.4 eV, thanks to the uniform 20% portion of the HF exchange integral. With these conventional functionals the errors tend to increase as the atomic nuclear charge becomes larger. This behavior can also be seen in the results of the LC-LH method. The LC-LH(1) method overestimated the core-excitation energies and had a MAE of 13.6 eV on average. This MAE is almost as large as that of time-dependent HF, 15.4 eV.[19] On the other hand, the LC-LH(0.48) method reproduced much more accurate core-excitation energies than LC-LH(1) did: the MAE of LC-LH(0.48) was 5.0 eV. LC-PSRSIC provided core-excitation energies more accurately than LC-LH could, although both of these methods employ the ratio *t* in eq 2 in the partition function *f*. This superior LC-PSRSIC result may be due to its parameter *a* depending on atomic species.

Valence, Rydberg, and Charge Transfer Excitation Energy Calculations. Next, we carried out TDDFT calculations on the valence-, Rydberg-, and charge transfer (CT)-excitation energies of typical molecules. We supposed that a method correcting for core-excitation energies would not be widely used if it gave inaccurate excitation energies except for core excitations.

Table 2 displays the calculated valence- and Rydberg-excitation energies of C_2H_2, C_2H_4, C_4H_6, CH_2O, and H_2O molecules. All methods except LC-LH(1) provided accurate valence-excitation energies with small MAEs of less than 0.4 eV, whereas LC-LH(1) had an MAE that was about three times worse than those of other LCs. LC-PSRSIC, LC-mRSIC, and LC-LH(0.48) gave especially small MAEs that were comparable to those of LC-BOP with no SIC. However, it should be noted that LH(0.48) had a bigger effect on the calculated valence-excitation energies of LC-BOP in comparison with PSRSIC and mRSIC. Table 2 also shows that LC-PSRSIC and LC-mRSIC gave accurate Rydberg-excitation energies very close to the LC-BOP values, while LC-LH(1) and LC-LH(0.48) significantly overestimated them. Similarly to valence excitations, PSRSIC and mRSIC hardly affected the excitation energies in comparison with LH(1) and LH(0.48). This result may come from the parameter *a* being dependent on nuclear charge in eq 25. PSRSIC had much less effect than mRSIC had on the valence- and Rydberg-excitation energies, probably because PSRSIC used the HF exchange integral to correct for self-interactions.

We also performed long-range CT-energy calculations on a C_2H_4—C_2F_4 dimer. Table 3 lists the lowest C_2F_4 $\pi \rightarrow C_2H_4$ π^* CT-excitation energies for intermolecular distances *R* from 5.0 to 10.0 Å. The CT-excitation energies at $R \rightarrow \infty$ were obtained by fitting the calculated CT energies $\omega_{CT}(R)$ for $R = 5.0-10.0$ Å to

$$\omega_{CT}(R) = c_0 - \frac{c_1}{R} \tag{26}$$

where c_0 corresponds to the CT-excitation energies at $R \rightarrow \infty$. The experimental c_0 value is 12.5 eV.[22] LC-PSRSIC and LC-mRSIC gave accurate c_0 values very close to that of LC-BOP, whereas LC-LH(1) and LC-LH(0.48) slightly overestimated c_0. In contrast to BOP and B3LYP, all LC methods produced reasonable values for c_1 (slightly greater than 1.0 au).

From the above results, we conclude that PSRSIC and mRSIC enable LC-TDDFT calculations to provide accurate core-excitation energies while preserving the accuracies of their valence-, Rydberg-, and CT-excitation energies.

Oscillator Strengths. To explore the reproducibility of electronic spectra, we also calculated the oscillator strengths

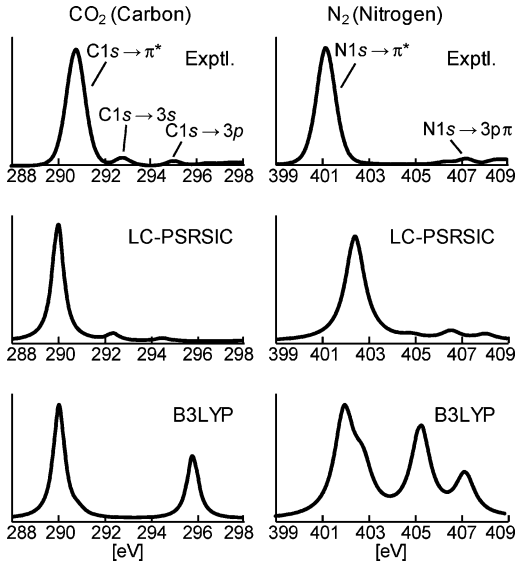

Figure 2. Experimental and theoretical absorption spectra of CO_2 and N_2 molecules. Theoretical spectra are obtained from LC-PSRSIC and B3LYP calculations.

(OSs) for the core, valence, and Rydberg excitations of a C_2H_4 molecule (Table 4). The table shows that LC-PSRSIC gives close OSs to LC-BOP ones even for core excitations. This indicates that PSRSIC has an insignificant effect on OSs. Compared to these OSs, B3LYP gave slightly higher OSs for core excitations, while lower OSs for valence and Rydberg excitations are estimated. Since the OSs of core excitations are underestimated by BOP, it may be due to the short-range Hartree−Fock exchange integral mixed in B3LYP. Figure 2 shows the experimental and theoretical absorption spectra of CO_2 in the range of 288−298 eV and those of N_2 in the range of 399−409 eV. For these spectra, the largest peaks were leveled to the same height. The experimental spectra were taken from the gas phase core-excitation database by Hitchcock.[59,60] The line shapes of the theoretical spectra were illustrated using Lorenzian-type functions with the half-bandwidths of 0.3 for CO_2 and 0.5 for N_2. The figure shows that LC-PSRSIC accurately reproduces the features of core-excitation spectra for both CO_2 and N_2. These features are in contrast to B3LYP ones, in which no excitations correspond to the experimental ones in these energy ranges.

Core-Ionization-Energy Calculations. Finally, we calculated core-ionization energies with the Δ-KS technique.[41] As mentioned in the Introduction, our previous study found that LC-mRSIC gave poor core-ionization energies.[25] Table 5 summarizes the calculated core-ionization energies. LC-PSRSIC gave accurate core-ionization energies, whereas LC-mRSIC did not: MAEs are 2.8 eV for LC-PSRSIC and 10.0 eV for LC-mRSIC. The results for LC-PSRSIC are comparable to those for LC-BOP, BOP, and B3LYP. This indicates that the exchange interactions between core and valence orbitals, which PSRSIC takes into account but mRSIC does not, play an important role in core-ionization energies. The LH methods also gave reasonably accurate core-ionization energies. It should be noted that large deviations are given for the core ionization energies of N_2. This is due to its high point group symmetry ($D_{\infty h}$). Since the 1s core-ionization of N_2 corresponds to removing an electron from the lowest σ orbital which spreads over two N atoms, it unnaturally removes 0.5 electrons from two N atoms. To improve the large deviations, a multiconfigurational or broken-symmetry approach may be required.

Conclusions

We modified the regional self-interaction (RSIC) method on the basis of the pseudospectral (PS) technique to obtain accurate core-excitation and core-ionization energies in long-range corrected (LC) DFT calculations.[21−23] In the RSIC method, self-interaction (SI) regions, where electrons interact only with themselves, are distinguished by the ratio of the Weizsäcker kinetic-energy density, and SI errors are reduced by substituting the exact self-exchange energy density for the exchange functional energy density in SI regions.

The original RSIC used the exact exchange energy density of the hydrogen 1s orbital,[24] and the previously proposed mRSIC method supplemented the exact exchange energy densities of 2s and higher hydrogen-like orbitals, which explicitly depend on the nuclear charge.[25] The new method, called "PSRSIC", adopts the HF exchange integral as the exact exchange energy density at each position by using the PS technique.[28] PSRSIC gives accurate core-excitation energies in LC-TDDFT calculations, and it maintains the accuracies of the valence-, Rydberg-, and charge transfer (CT)-excitation energies of TDDFT and the core-ionization energies of DFT calculations.

The LC-TDDFT calculations showed that, like mRSIC, PSRSIC significantly improves the accuracies of the core-excitation energies: the mean absolute error (MAE) of LC-PSRSIC, 1.2 eV, is about 20 times smaller than that of LC calculations with no SI corrections (SIC), 23.1 eV. We also found that LC-PSRSIC has no negative effect on valence-, Rydberg-, and CT-excitation energies in LC-TDDFT calculations. Furthermore, unlike the LC-mRSIC method, LC-PSRSIC does not have a negative effect on core-ionization energies.

Consequently, we conclude that this new method for obtaining accurate core-excitation energies in LC-TDDFT calculations can also maintain the accuracies of valence-, Rydberg-, and CT-excitation energies and in core-ionization energies in LC-DFT calculations. However, PSRSIC still has arbitrariness in determining the parameter a in eq 25. We suppose that this is due to the discrepancy in SI regions for different types of atoms, but we must leave this question open for the time being.

In this study, we have shown excited state calculations besides core ionization energies. We calculated the standard enthalpies

TABLE 5: Core-Ionization Energies (in eV) of CO_2, N_2, and HF Molecules and Ne Atom Calculated by Δ-KS with BOP, LC-BOP, LC-mRSIC, LC-PSRSIC, B3LYP, and LH Functionals with cc-pVTZ Plus Rydberg Basis Functions[a]

molecule	BOP	LC-BOP	LC-mRSIC	LC-PSRSIC	B3LYP	LC-LH(1)	LC-LH(0.48)	exptl
CO_2	297.2 (−0.3)	297.1 (−0.4)	292.2 (−5.3)	296.0 (−1.5)	298.0 (+0.5)	299.1 (+1.6)	298.6 (+1.1)	297.5[b]
N$_2$	401.6 (−8.3)	401.6 (−8.3)	390.1 (−19.8)	406.7 (−3.2)	405.3 (−4.6)	415.8 (+5.9)	409.0 (−0.9)	409.9[c]
H**F**	693.7 (−0.4)	693.1 (−1.0)	687.1 (−7.0)	691.6 (−2.5)	693.8 (−0.3)	692.4 (−1.7)	693.2 (−0.9)	694.1[d]
Ne	869.2 (−1.1)	868.7 (−1.6)	862.5 (−7.8)	866.1 (−4.2)	869.4 (−0.9)	867.9 (−2.4)	868.7 (−1.6)	870.3[e]
MAE[f]	2.5	2.8	10.0	2.8	1.6	2.9	1.1	

[a] Errors with respect to the experimental data are shown in parentheses. The atoms whose 1s electrons are removed are in boldface. [b] Ref 61. [c] Ref 53. [d] Ref 55. [e] Ref 56. [f] Mean absolute errors from the experimental data.

of formation of G2-1 set[62] and found that LC-PSRSIC gave much poorer results than conventional functionals did: the MAEs are 3.6, 2.9, 9.9, and 29.7 kcal/mol for BOP, B3LYP, LC-BOP, and LC-PSRSIC, respectively. This may be due to the arbitrariness of parameter a in eq 25 which determines SI regions. Since this parameter was determined to give accurate core excitation energies, it is not well applied to ground state property calculations. To obtain a so-called universal functional, the arbitrariness in determining SI regions has to be removed from this method. There is room for further investigation.

Acknowledgment. The calculations were partly performed at the RIKEN Integrated Cluster of Clusters (RICC) System. This study was supported by the Ministry of Education, Culture, Sports, Science and Technology (grants no. 20038012 and 20350002) and the Core Research for Evolutional Science and Technology Program of the Japan Science and Technology Agency (JST). One of the researchers (TT) was supported by contributions from Hitachi Chemical Co., Ltd. and Toshiba Co., Ltd.

Appendix

TDDFT Equation for PSRSIC

Considering the linear response to an oscillator perturbation, the TDDFT equation is obtained as a non-Hermitian eigenvalue equation[5,8,9]

$$\begin{pmatrix} \mathbf{A} & \mathbf{B} \\ \mathbf{B}^* & \mathbf{A}^* \end{pmatrix}\begin{pmatrix} \mathbf{X} \\ \mathbf{Y} \end{pmatrix} = \omega\begin{pmatrix} \mathbf{1} & \mathbf{0} \\ \mathbf{0} & -\mathbf{1} \end{pmatrix}\begin{pmatrix} \mathbf{X} \\ \mathbf{Y} \end{pmatrix} \tag{A1}$$

where the eigenvalues $\boldsymbol{\omega}$ correspond to the excitation energies and eigenfunctions $\mathbf{X}$ and $\mathbf{Y}$ to excitation vectors. The matrix elements of $\mathbf{A}$ and $\mathbf{B}$ are

$$A_{ai,bj} = (\varepsilon_a - \varepsilon_i)\delta_{ab}\delta_{ij} + K_{ai,bj} \tag{A2}$$

$$B_{ai,bj} = K_{ai,jb} \tag{A3}$$

We use the subscripts i and j for occupied orbitals and a and b for virtual orbitals. $\mathbf{K}$ for the general MOs p, q, r, and s is written as

$$K_{pq,rs} = \frac{\partial F_{pq\sigma}}{\partial P_{rs\tau}} = (p_\sigma q_\sigma|s_\tau r_\tau) - a_{\mathrm{HF}}\delta_{\sigma\tau}(p_\sigma r_\tau|s_\tau q_\sigma) + \frac{\partial^2 E^{\mathrm{DFT}}}{\partial P_{rs\tau}\partial P_{pq\sigma}} \tag{A4}$$

$\mathbf{F}$ and $\mathbf{P}$ are Fock and density matrices, and σ and τ are electron spins. For the PSRSIC functional, $\mathbf{K}$ becomes

$$K^{\mathrm{PSRSIC}}_{pq,rs} = (p_\sigma q_\sigma|s_\tau r_\tau) + \int\left[\frac{\partial f(\mathbf{r})}{\partial P_{rs\tau}}\left(\frac{\partial \varepsilon_x^{\mathrm{SI}}(\mathbf{r})}{\partial P_{pq\sigma}} - \frac{\partial \varepsilon_x^{\mathrm{DFT}}(\mathbf{r})}{\partial P_{pq\sigma}}\right) + f(\mathbf{r})\frac{\partial^2 \varepsilon_x^{\mathrm{SI}}(\mathbf{r})}{\partial P_{rs\tau}\partial P_{pq\sigma}} + (1 - f(\mathbf{r}))\frac{\partial^2 \varepsilon_x^{\mathrm{DFT}}(\mathbf{r})}{\partial P_{rs\tau}\partial P_{pq\sigma}} + \frac{\partial(\varepsilon_x^{\mathrm{SI}}(\mathbf{r}) - \varepsilon_x^{\mathrm{DFT}}(\mathbf{r}))}{\partial P_{rs\tau}}\frac{\partial f(\mathbf{r})}{\partial P_{pq\sigma}} + (\varepsilon_x^{\mathrm{SI}}(\mathbf{r}) - \varepsilon_x^{\mathrm{DFT}}(\mathbf{r}))\frac{\partial^2 f(\mathbf{r})}{\partial P_{rs\tau}\partial P_{pq\sigma}}\right]d\mathbf{r} + \frac{\partial^2 E_c^{\mathrm{DFT}}}{\partial P_{rs\tau}\partial P_{pq\sigma}} \tag{A5}$$

The first and last terms are the contributions from the Coulomb energy and correlation energy, and the other terms are the contributions from the exchange energy. The integration over $\mathbf{r}$ is performed numerically. In the MO basis, the first derivatives of f, $\varepsilon_x^{\mathrm{SI}}$ and $\varepsilon_x^{\mathrm{DFT}}$ in eq A5, are equivalent to their Fock elements. The second derivative of $\varepsilon_x^{\mathrm{DFT}}$ is obtained in the conventional way, and that of f is obtained in the same way as is done for the meta-GGA functionals. The second derivative of $\varepsilon_x^{\mathrm{SI}}$ is like the second term in eq A4 but integrated over only one spatial index

$$\frac{\partial^2 \varepsilon_x^{\mathrm{SI}}(\mathbf{r})}{\partial P_{rs\tau}\partial P_{pq\sigma}} = -\delta_{\sigma\tau}p_\sigma(\mathbf{r})r_\tau(\mathbf{r})\int\frac{s_\tau(\mathbf{r}_2)q_\sigma(\mathbf{r}_2)}{|\mathbf{r}_2 - \mathbf{r}|}d\mathbf{r}_2 \tag{A6}$$

Supporting Information Available: Core-excitation energies from X-1s orbitals (X = C of C_2H_4 and CO_2, N of N_2 and NH_3, O of CO_2 and H_2O, F of HF and F_2, and Ne) calculated by TDDFT with LC-PSRSIC for various a values. Cc-pVTZ plus Rydberg basis functions were used. The differences from the experimental data and the mean values of them are also shown. This material is available free of charge via the Internet at http://pubs.acs.org.

References and Notes

(1) Shirai, S.; Yamamoto, S.; Hyodo, S. *J. Chem. Phys.* **2004**, *121*, 7586.
(2) Kuramoto, K.; Ehara, M.; Nakatsuji, H.; Kitajima, M.; Tanaka, H.; De Fanis, A.; Tamenori, Y.; Ueda, K. *J. Electron Spectrosc. Relat. Phenom.* **2005**, *142*, 253.
(3) Kuramoto, K.; Ehara, M.; Nakatsuji, H. *J. Chem. Phys.* **2005**, *122*, 014304.
(4) Ehara, M.; Kuramoto, K.; Nakatsuji, H.; Hoshino, M.; Tanaka, T.; Kitajima, M.; Tanaka, H.; De Fanis, A.; Tamenori, Y.; Ueda, K. *J. Chem. Phys.* **2006**, *125*, 114304.
(5) Casida, M. E. In *Recent Advances in Density Functional Methods*; Chong, D. P., Ed.; World Scientific: Singapore, 1995; Pt. I, Chapter 5, pp 155−192.
(6) Bauernschmitt, R.; Ahlrichs, R. *Chem. Phys. Lett.* **1996**, *256*, 454.
(7) Stratmann, R. E.; Scuseria, G. E.; Frisch, M. J. *J. Chem. Phys.* **1998**, *109*, 8218.
(8) Hirata, S.; Head-Gordon, M. *Chem. Phys. Lett.* **1999**, *314*, 291.
(9) Hirata, S.; Head-Gordon, M.; Bartlett, R. J. *J. Chem. Phys.* **1999**, *111*, 10774.
(10) Jamorski, C.; Casida, M. E.; Salahub, D. R. *J. Chem. Phys.* **1996**, *104*, 5134.
(11) Casida, M. E.; Jamorski, C.; Casida, K. C.; Salahub, D. R. *J. Chem. Phys.* **1998**, *108*, 4439.
(12) van Gisbergen, S. J. A.; Snijders, J. G.; Baerends, E. J. *J. Chem. Phys.* **1995**, *103*, 9347.
(13) Imamura, Y.; Nakai, H. *Chem. Phys. Lett.* **2006**, *419*, 297.
(14) Imamura, Y.; Otsuka, T.; Nakai, H. *J. Comput. Chem.* **2007**, *28*, 2067.
(15) Imamura, Y.; Nakai, H. *Int. J. Quantum Chem.* **2007**, *107*, 23.
(16) Nakata, A.; Imamura, Y.; Ostuka, T.; Nakai, H. *J. Chem. Phys.* **2006**, *124*, 094105.
(17) Tsuchimochi, T.; Kobayashi, M.; Nakata, A.; Imamura, Y.; Nakai, H. *J. Comput. Chem.* **2008**, *29*, 2311.

(18) Thompson, A.; Saha, S.; Wang, F.; Tsuchimochi, T.; Nakata, A.; Imamura, Y.; Nakai, H. *Bull. Chem. Soc. Jpn.* **2009**, *82*, 187.
(19) Nakata, A.; Imamura, Y.; Nakai, H. *J. Chem. Phys.* **2006**, *125*, 064109.
(20) Nakata, A.; Imamura, Y.; Nakai, H. *J. Chem. Theory Comput.* **2007**, *3*, 1295.
(21) Iikura, H.; Tsuneda, T.; Yanai, T.; Hirao, K. *J. Chem. Phys.* **2001**, *115*, 3540.
(22) Tawada, Y.; Tsuneda, T.; Yanagisawa, S.; Yanai, T.; Hirao, K. *J. Chem. Phys.* **2004**, *120*, 8425.
(23) Song, J. W.; Watson, M. A.; Nakata, A.; Hirao, K. *J. Chem. Phys.* **2008**, *129*, 184113.
(24) Tsuneda, T.; Kamiya, M.; Hirao, K. *J. Comput. Chem.* **2003**, *24*, 1592.
(25) Nakata, A.; Tsuneda, T.; Hirao, K. *J. Comput. Chem.* **2009**, *30*, 2583.
(26) Dreizler, R. M.; Gross, E. K. U. In *Density-Functional Theory: An Approach to the Quantum Many-Body Problem*; Springer-Verlag: Berlin, Heidelberg, 1990.
(27) Tao, J. *J. Chem. Phys.* **2001**, *115*, 3519.
(28) Langlois, J. M.; Muller, R. P.; Coley, T. R.; Goddard, W. A., III; Ringnalda, M. N.; Won, Y.; Friesner, R. A. *J. Chem. Phys.* **1990**, *92*, 7488.
(29) Imamura, Y.; Takahashi, A.; Nakai, H. *J. Chem. Phys.* **2007**, *126*, 034103.
(30) Seidl, A.; Görling, A.; Vogl, P.; Majewski, J. A.; Levy, M. *Phys. Rev. B* **1996**, *53*, 3764.
(31) Neumann, R.; Nobes, R. H.; Handy, N. C. *Mol. Phys.* **1996**, *87*, 1.
(32) Jaramillo, J.; Scuseria, G. E.; Ernzerhof, M. *J. Chem. Phys.* **2003**, *118*, 1068.
(33) Henderson, T. M.; Janesko, B. G.; Scuseria, G. E. *J. Phys. Chem. A* **2008**, *112*, 12530.
(34) Della Sala, F.; Görling, A. *J. Chem. Phys.* **2001**, *115*, 5718.
(35) Bahmann, H.; Rodenberg, A.; Arbuznikov, A. V.; Kaupp, M. *J. Chem. Phys.* **2007**, *126*, 011103.
(36) Janesko, B. G.; Scuseria, G. E. *J. Chem. Phys.* **2008**, *128*, 084111.
(37) Janesko, B. G.; Scuseria, G. E. *J. Chem. Phys.* **2007**, *127*, 164117.
(38) Adamson, R. D.; Dombroski, J. P.; Gill, P. M. W. *J. Comput. Chem.* **1999**, *20*, 921.
(39) Dunning, T. H., Jr. *J. Chem. Phys.* **1989**, *90*, 1007.
(40) Dunning, T. H.; Hay, P. J. *Methods of Electronic Structure Theory*; Scheafer, H. F., III, Ed.;Plenum Press: New York, 1977; Vol. 3.
(41) Chong, D. P. *J. Electron Spectrosc. Relat. Phenom.* **2005**, *148*, 115.
(42) Chong, D. P.; Takahata, Y. *Chem. Phys. Lett.* **2006**, *418*, 286.
(43) Murray, C. W.; Handy, N. C.; Laming, G. J. *Mol. Phys.* **1993**, *78*, 997.
(44) *Numerical recipes in Fortran 77*, 2nd ed.; Cambridge University Press: New York, 1992.
(45) Becke, A. D. *Phys. Rev. A* **1988**, *38*, 3098.
(46) Tsuneda, T.; Suzumura, T.; Hirao, K. *J. Chem. Phys.* **1999**, *110*, 10664.
(47) Becke, A. D. *J. Chem. Phys.* **1993**, *98*, 5648.
(48) Lee, C.; Yang, W.; Parr, R. G. *Phys. Rev. B* **1988**, *37*, 785.
(49) Schmidt, M. W.; Baldridge, K. K.; Boatz, J. A.; Elbert, S. T.; Gordon, M. S.; Jensen, J. H.; Koseki, S.; Matsunaga, N.; Nguyen, K. A.; Su, S.; Windus, T. L.; Dupuis, M.; Montgomery, J. A. *J. Comput. Chem.* **1993**, *14*, 1347.
(50) Gordon, M. S.; Schmidt, M. W. *Theory and Applications of Computational Chemistry: the first forty years*; Elsevier: Amsterdam, 2005; pp 1167−1189.
(51) Hu, C.-H.; Chong, D. P. *Chem. Phys. Lett.* **1996**, *262*, 729.
(52) Ma, Y.; Chen, C. T.; Meigs, G.; Randall, K.; Sette, F. *Phys. Rev. A* **1991**, *44*, 1848.
(53) Ohno, M.; Decleva, P.; Fronzoni, G. *Surf. Sci.* **1993**, *284*, 372.
(54) Niu, A. F.; Zhang, Y.; Zhang, W. H.; Li, J. M. *Phys. Rev. A* **1998**, *57*, 1912.
(55) Hitchcock, A. P.; Brion, C. E. *J. Phys. B: At. Mol. Phys.* **1981**, *14*, 4399.
(56) Romberg, R.; Kassühlke, B.; Wiethoff, P.; Menzel, D.; Feulner, P. *Chem. Phys.* **2003**, *289*, 69.
(57) Dressler, R.; Allan, M. *J. Chem. Phys.* **1987**, *87*, 4510.
(58) Serrano-Andrés, L.; Merchán, M.; Nebot-Gil, I.; Lindh, R.; Roos, B. O. *J. Chem. Phys.* **1993**, *98*, 3151.
(59) Hitchcock, A. P. Gas Phase Core Excitation Database at http://unicorn.mcmaster.ca/corex/cedb-title.html.
(60) McLaren, R.; Clark, S. A.; Ishii, I.; Hitchcock, A. P. *Phys. Rev. A* **1987**, *36*, 1683.
(61) Sivkov, V. N.; Akimov, V. N.; Vinogradov, A. S.; Zimkina, T. M. *Opt. Spectrosc.* **1984**, *57*, 160.
(62) Curtiss, L. A.; Raghavachari, K.; Redfern, P. C.; Pople, J. A. *J. Chem. Phys.* **1997**, *106*, 1063.

JP909915D